Electronic Supplementary Material (ESI) for Photochemical & Photobiological Science

Electronic Supplementary Information to:

Bis-Semi-Quinone (bi-radical) Formation by Photoinduced Proton Coupled Electron Transfer in Covalently linked Catechol-Quinone systems: Aviram's Hemi-Quinones Revisited

by

Nguyên Vân Anh and René M. Williams*

Molecular Photonics group, van't Hoff Institute for Molecular Sciences (HIMS), Faculty of Science, Universiteit van Amsterdam, Science Park 904, 1098 XH Amsterdam, The Netherlands

Manuscript for special issue for Prof. Dr. Kurt Schaffner

Content:

Molecular structures of compounds used

HPLC of **BQ**

UV-Vis of **Q** in veratrole, anisole, toluene, methylcyclohexane

UV-Vis of intermolecular complexes of **Q** and **C**

IR of intermolecular complexes of **Q** and **C**

ns-TA of **Q** and **BQ** (triplet formation)

ns-TA of **Q** in veratrole ($\mathbf{Q}^{-\cdot}$ formation)

ns-TA of **HQ** in MCH (bis semiquinone radial formation) + kinetics+ and of model systems

reactivity of quinones with thiols probed with IR and UV-Vis

experimental setup, procedures and sample handling

Molecular structures of compounds used

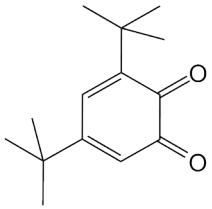

3,5 di-tert-butyl o-benzoquinone (**Q**)

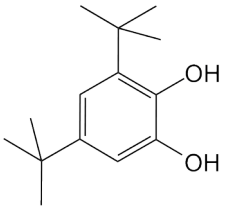

3, 5 di-tert butyl catechol (**C**)

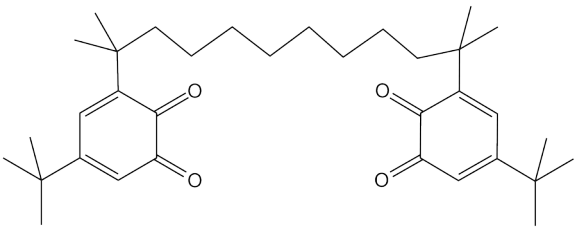

6,6'-(2,11-dimethyldodecane-2,11-diyl)bis(4-tert-butylcyclohexa-3,5-diene-1,2-dione)

(**BQ**)

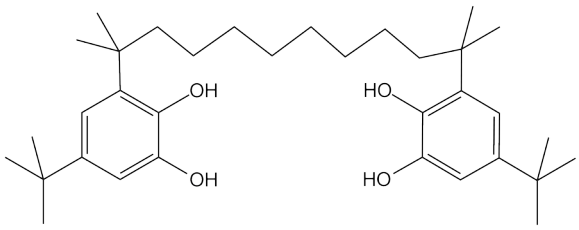

6,6'-(2,11-dimethyldodecane-2,11-diyl)bis(4-(tert-butyl)benzene-1,2-diol)

(**BC**)

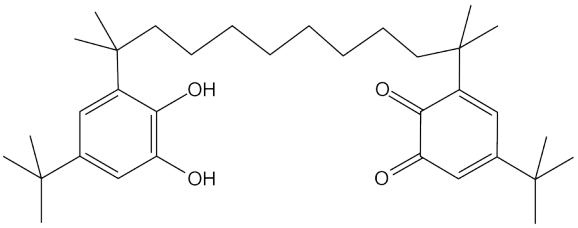

Symmetric hemiquinone (**HQ**)

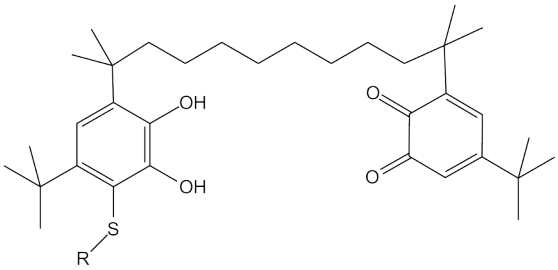

Asymmetric hemiquinone (**AHQ**)

Scheme S1: Lewis structures of studied compounds.

HPLC of BQ

The purity of **BQ** that was synthesized in 1983 at IBM was assessed with HPLC-MS. Only one component eluted at 4.24 min. from which a purity of 99.9 % was determined. The UV-Vis spectrum (corresponding to the HPLC peak at 4.24 min.) shows the typical spectrum of quinone derivatives, with a broad band centered at 405 nm and a sharp strong band at 239 nm.

The mass spectrum (corresponding to the HPLC- peak at 4.24 min) showed a major peak that can be attributed to the protonated molecule at 523.31 [**BQ**-H]$^+$. Peaks at 540.30, 568.40 and 1061.92 were also observed and are most likely due to the hydrated, acid complex and dimeric (and hydrated) species.

The HPLC-MS experiments were carried out with a Finnigan LXQ Ion Trap Mass Spectrometer coupled with a Finnigan Surveyor Plus HPLC system equipped with a Xterra-C18 column (50 mm × 2.1 mm; 3.5μm particle size). A gradient between solvent A (H_2O/0.1% HCOOH) and solvent B (CH_3CN/0.1% HCOOH) was used as eluent. The electronspray ionization mass spectra (ESI) were scanned in a full range (*m/z* = 100.00 – 2000.00). The detection range for HPLC-UV/Vis determination was between 200 and 600 nm.

UV-Vis of Q in veratrole, anisole, toluene, methylcyclohexane

In order to separate the effects of hydrogen bonding and charge transfer, different donors which have a very similar structure to the catechol compound were used in combination with **Q**. Figure S**1** presents the UV-Vis absorption of **Q** in different electron donating solvents, showing the charge transfer absorption characteristics of **Q** in different media.

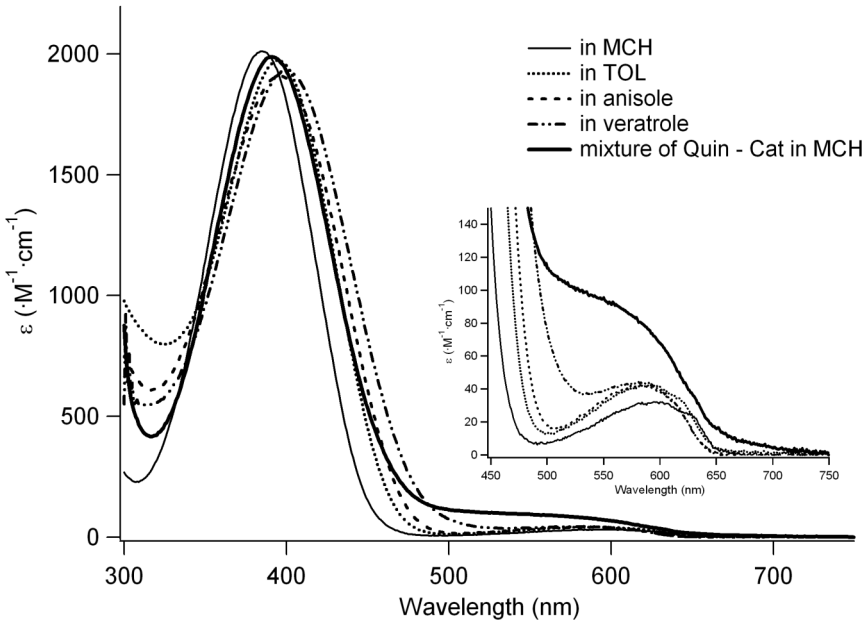

Figure S1. Absorption spectra of 3,5 di-tert butyl *o*-benzoquinone (Quin = **Q**) in MCH (solid line), TOL (toluene, dotted line), anisole (dashed line) and veratrole (dash-dot-dot line), and of the mixture of Quin and 3,5 di-tert butyl catechol (Cat = **C**) in MCH (solid bold line)

The spectra show that the π - π* band (at ca. 388 nm) of **Q** shifts to the red side and the n - π* transition band shifts to the blue side in toluene, anisole and veratrole. The red-shift in the π - π* band could be due to i) the π - π interaction between Quin and these solvents and ii) the higher polarity of these solvents comparing to MCH. Taking into account that veratrole and catechol have similar donor strengths indicates that in the covalently linked complex not only charge transfer is present (indicated by the new absorption around 500 nm in veratrole) but also hydrogen bonding. The absorption of the **HQ** in MCH in the 500 -600 nm region is much more intense.

UV-Vis of intermolecular complexes of Q and C

Here we give difference absorption spectra (as well as normalized absorption spectra) of the intermolecular complex between **Q** and **C** in methylcyclohexane.

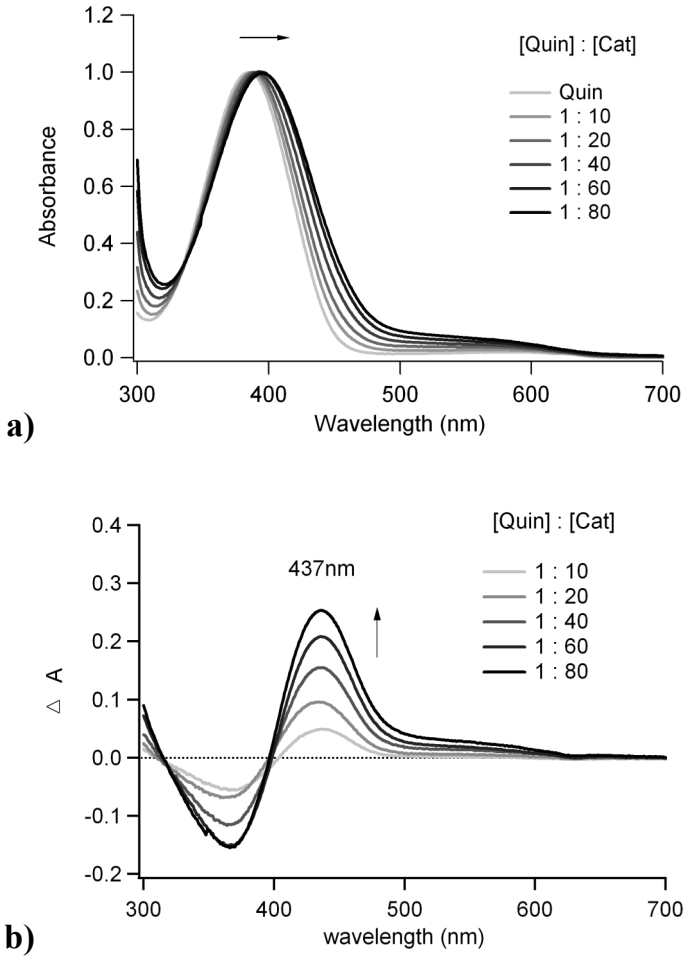

Figure S2 The normalized UV-Vis absorption spectra (a) and the difference absorption (b) of the different ratio mixtures between **Q** and **C** (Quin-Cat) in methylcyclohexane (MCH), [**Q**] = 5×10^{-4} M.

There are two possible complexes, the sandwich complex and the coplanar complex (see the structures below). In the sandwich complex, two rings are in two parallel planes whereas in the co-planar one, these rings are in a single plane so that the two carbonyl and hydroxyl groups are opposite in pair. (See reference 16)

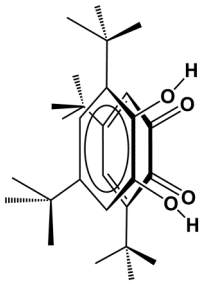

Sandwich complex (SC)

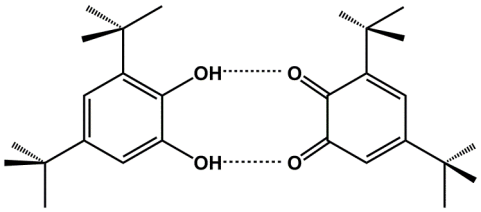

Co-planar complex (CC)

Figure S2b shows that the ΔA between 400 and 600 nm increases with an increase of the ratio of catechol and quinone concentrations.

IR of intermolecular complexes of Q and C

We show the IR spectra of **BC** and the mixture of **BC** and **BQ** (= **HQ)** (again) in figure **S3a**. The IR spectroscopy of Cat (= **C)** and mixture and **C** and Quin (= **Q)** (figure **S3b**) is shown for comparison.

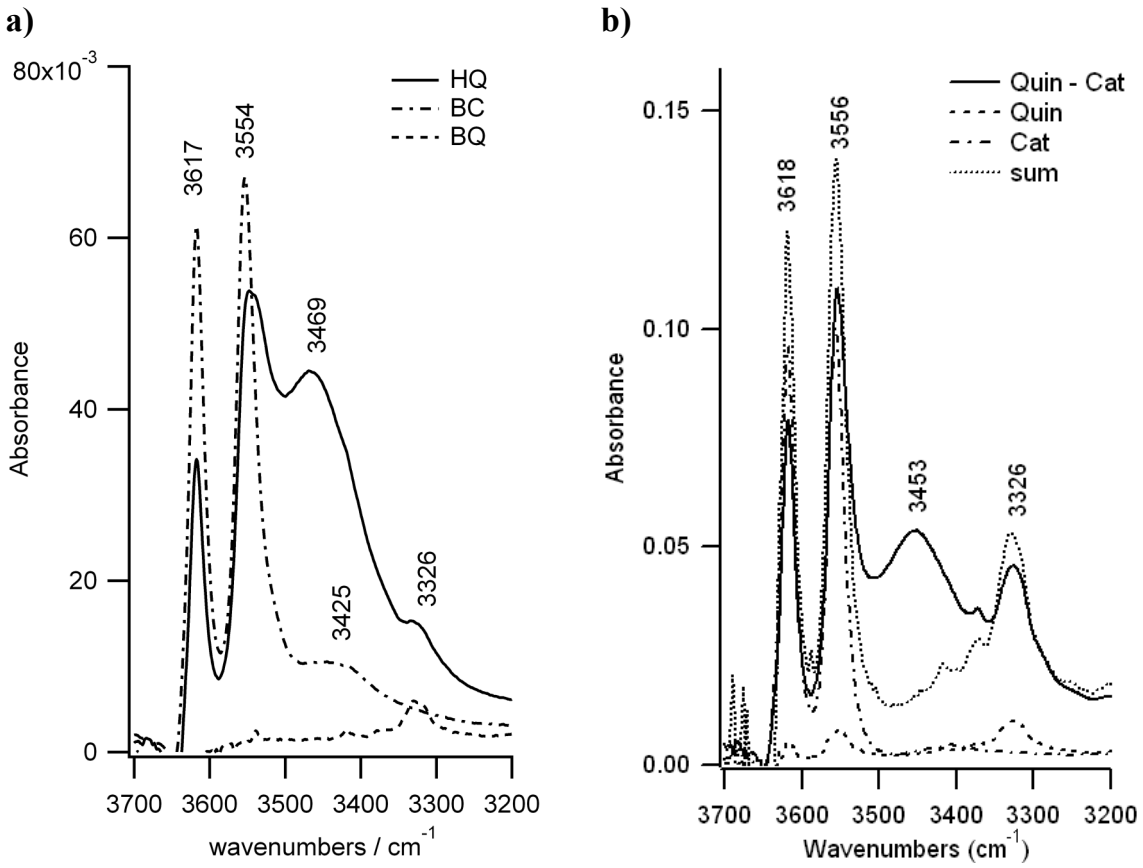

Figure S3. *The FT-IR spectra of the OH stretching vibrations of the catechol-quinone systems (a)* **[BC]** = **[BQ]** = 2×10^{-3} *M, and (b) the* **Q-C** *systems* **[C]** = 5×10^{-3} *M,* **[Q]** = 25×10^{-3} *M (b) in* CCl_4*, 1 mm cell thickness.*

The IR spectroscopy of the reference system, the **C** and the mixture of **C** and **Q**, presented very similar phenomena, indicating the complex formation between **C** and **Q** (figure **S3b**). These results relate very well to previous work. After the addition of the **Q** solution, a new peak appeared at 3456 cm^{-1} attributed to the stretching vibration of the O-H group which is bound by the C=O group of **Q**. When the ratio [**Q**] : [**C**] increases, the intensity of the absorption peak corresponding to the bound OH group increases whereas that of the "free" OH group decreases indicating the interaction

between **C** and **Q**. The peak at 3326 cm^{-1} in figure **S3a** and **S3b** is of the overtone of C=O stretch which is at 1663 cm^{-1}.

In summary, the covalent linkage between the catechol and the quinone units in the hemiquinone compound makes the hydrogen bond more favorable in comparison to the **Q** and **C** mixture (*i.e.* high local concentration). We obtained clear signatures for hydrogen bond formation as well as indication that some free OH is still present.

ns-TA of Q and BQ (triplet formation)

Figure S4 shows the transient absorption (TA) spectroscopy of **Q** and **BQ** on the nanosecond time scale. The spectra are virtually identical, presenting a band centered at 523 nm, which is attributed to the triplet absorption of o-benzoquinone derivatives with a long life time (ca. 280 ns for BQ and ca. 300 ns for Quin).

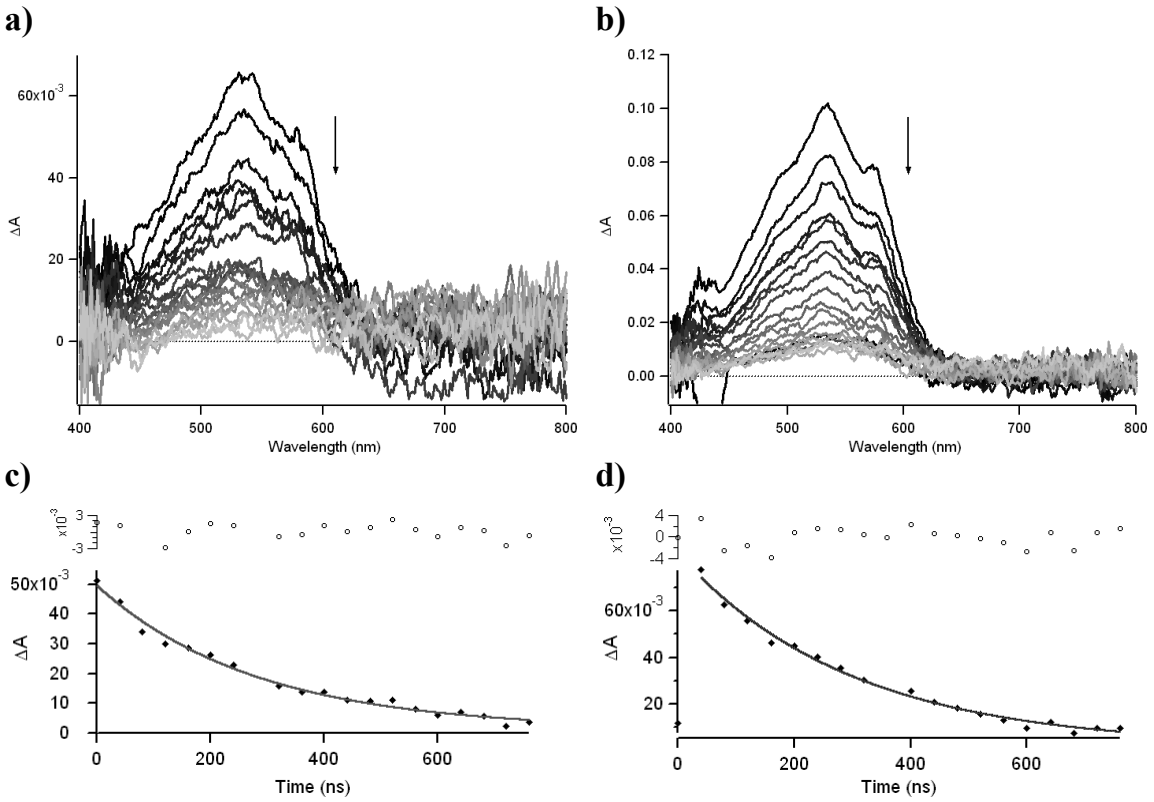

Figure S4. *The nanosecond transient absorption spectra of (a) of* **BQ** *(1 x 10^{-3} M), (b)* **Q** *(5 × 10^{-3} M) in MCH and corresponding decays (c) and (d) upon 440 nm excitation, 40 ns incremental time delay; the solutions were de-aerated by Ar bubbling for 20 minutes; laser power after sample holder was ca. 1.2. mJ/pulse for* **BQ** *and ca. 0.5 mJ for* **Q**.

ns-TA of Q in veratrole ($Q^{-\cdot}$ formation)

To get more information about the electron transfer process, we obtained ns-TA spectra of **Q** in two different electron donating solvents, anisole and veratrole; figure S5 shows the results.

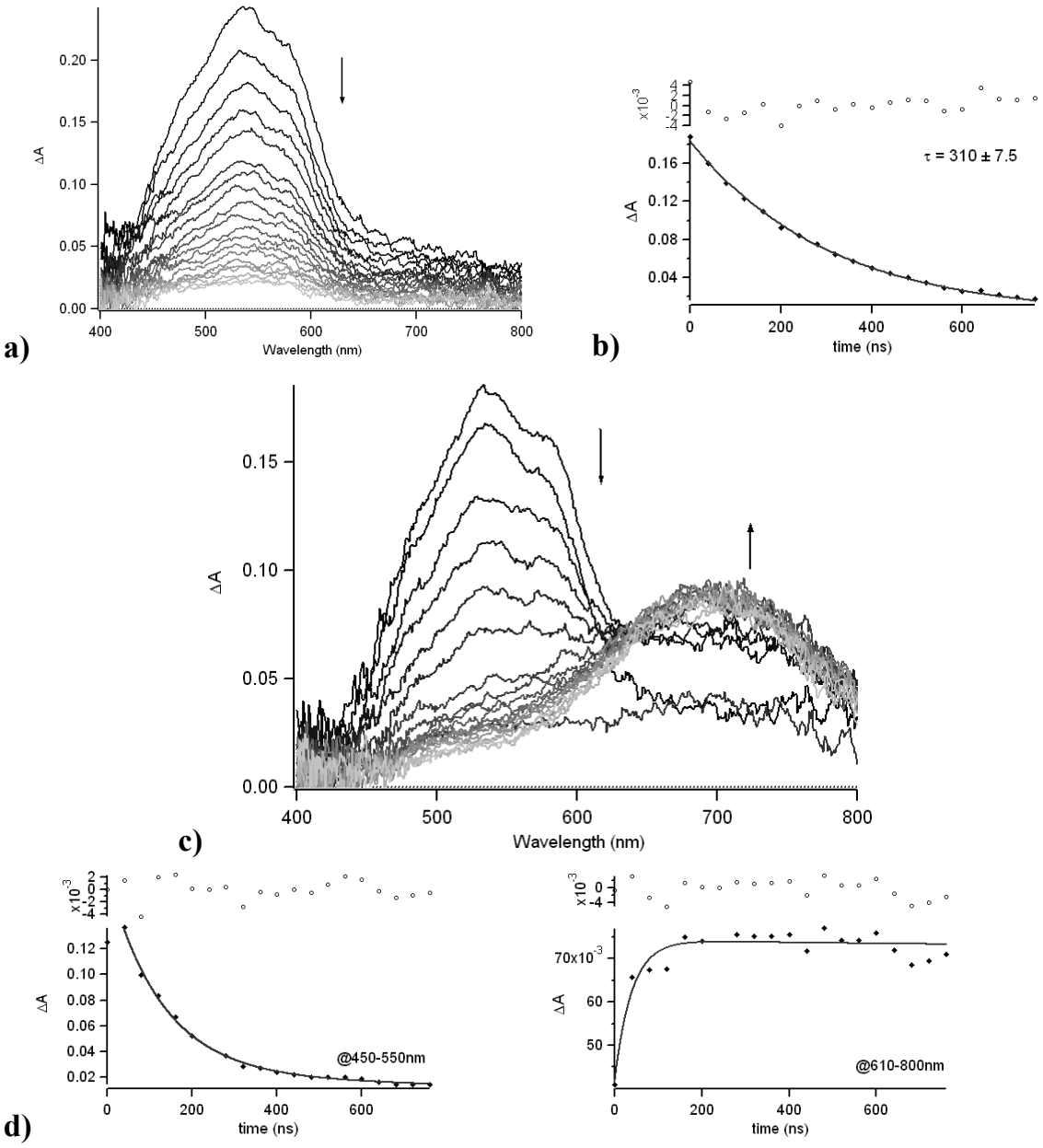

Figure S5. *The nanosecond transient absorption of* **Q** *(5 x 10^{-3} M) in anisole (a), and its time profile (b) and veratrole (c), and its time profile (d), upon 440 nm excitation wavelength, 1.2 mJ laser power after sample holder, 40 ns incremental time delay, degassed by Ar-bubbling in 30 minutes.*

For anisole, we observed the typical triplet state absorption of o-benzoquinone in the region 400 – 600 nm with a life time of ca. 300 ns, the same as the life time of **Q** in MCH. With the stronger electron donor, veratrole, we clearly observed the charge transfer process, characterized by the decay of the band at 500 nm and the formation of the broad band at 700 nm which is characteristic for the *o*-quinone radical anion species.

ns-TA of HQ in MCH (bis semiquinone radial formation) + kinetics and of model systems

The transient absorption spectra (figure S6) of the hemiquinone (**HQ**) and of the **C-Q** mixture show different features, as compared to **BQ** or **Q**. The 500 – 600 nm band attributed to the triplet-excited state of the o-quinone derivatives was not present, and a new band is observed centered at 720 nm. This band is attributed to the semiquinone radical.

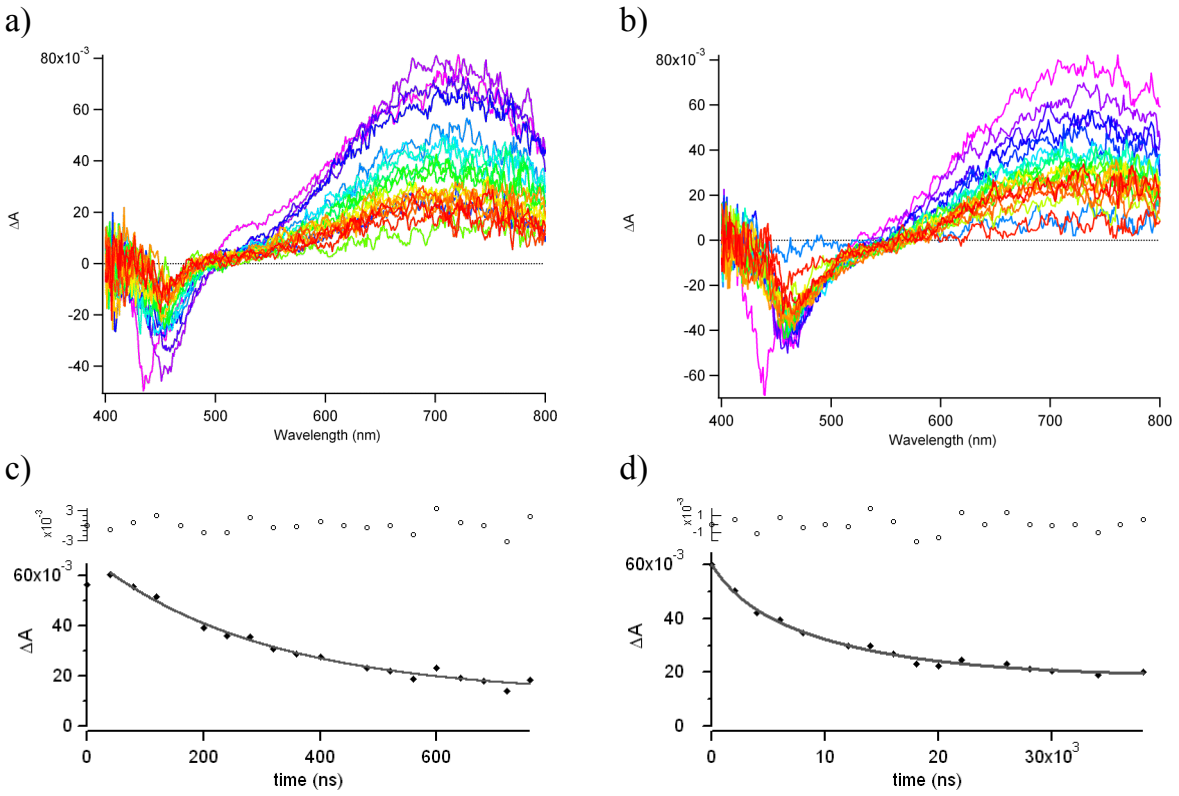

Figure S6. *The nanosecond transient absorption of* **HQ** *(a) with its time profile (c) and mixture of* **Q** *and* **C** *(b), and its time profile (d) upon 440 nm excitation, laser power was ca. 1.2 mJ/pulse; degassed by Ar bubbling in 20 minutes; the incremental delay was 40 ns for* **HQ** *and 2000 ns for the Quin-Cat mixture;* [**HQ**] *= (1 x* 10^{-3} *M),* [**Q**] *=* 2.5×10^{-3} *M and* [**C**] *=* 1×10^{-1} *M.*

The main difference in the ns-TA data of the covalently linked *o*-benzoquinone-catechol system and the non-covalently linked system is the kinetics. The mixture **C-Q**

showed two long lifetimes (ca. 91 μs) and (ca. 6.1 μs) upon biexponential fitting. However, this reference system can also be described by second order decay kinetics, which implies some direct recombination and some diffusion controlled recombination coming from some primary PCET products that escape from the solvent cage.

For the linked system, the decay of the signal is also bi-exponential but the lifetimes are shorter (300 ns and 18 μs). We attribiute the latter to the one H-bonded population.

Table S1. *The triplet state lifetimes (top) and CT/radical pair-lifetimes (lower part) obtained with ns-TA of* **Q** *with different donors and of* **BQ** *and* **HQ**

	τ_T (ns)	τ_{CR1} (ns)	τ_{CR2} (ns)
Q in MCH	310		
Q in Tol	330		
Q in anisole	320		
BQ in MCH	300		
Q in veratrole	127 (87%)	1650 (13%)	
Q-C in MCH		6100 (51%)	91000 (49%)
HQ in MCH		300 (81%)	18000 (19%)

Reactivity of quinones with thiols probed by IR

The reactivity of **Q** was studied by the addition of thiol compounds. The reaction between **Q** and thiol compounds also could be detected with IR spectroscopy, probing the reactivity of *o*-benzoquinone derivatives. The investigation of the reactivity of **Q** with thiols was carried out by mixing the solutions of **Q** and thiols in a 1:1 molar ratio. Two thiols with different acidity were used: mercaptopropionic acid (MPA- figure S7) and n-propylmercaptan (NPM – figure S8).

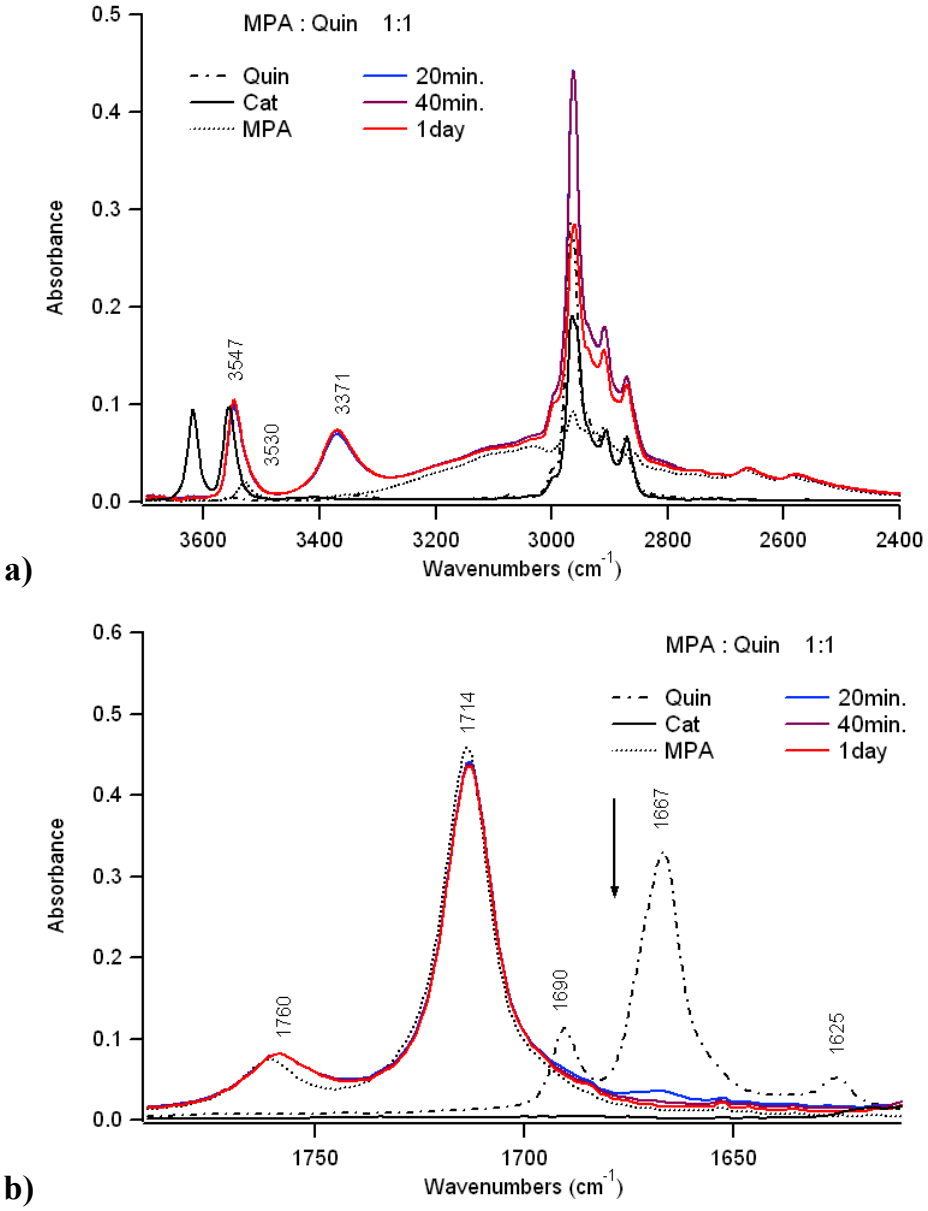

Figure S7. *FT-IR spectra of the mixture of mercaptopropionic acid (MPA) and Quin (= **Q**) versus time in the OH vibration band region (a) and C=O vibration band region (b)* $[MPA]_o = [\mathbf{Q}]_o = 5 \times 10^{-3}$ *M. The cell thickness is 1 mm.* CCl_4 *was used as solvent. The IR spectrum of catechol (**C**) is given for comparison.*

For pristine MPA the spectrum showed the typical monomer peak at 3530 cm^{-1} of the OH vibration of the acid (figure S7a). A characteristic broad band in the range of 3300 – 2500 cm^{-1}, which overlaps the C – H stretching vibrations is assigned as O–H stretching absorption of a dimeric carboxylic acid. The bands at 1761 cm^{-1} and 1714

cm^{-1} (figure S7b) correspond to the monomer and dimer C=O stretching modes, respectively, of the acid group in MPA.

When *o*-benzoquinone was added, the bands at 3547 cm^{-1} and at 3371 cm^{-1} (figure S7a) immediately appeared indicating the reaction of o-benzoquinone with MPA. These bands indicate two different intramolecular hydrogen bond OH stretch vibrations of the catechol. The thiol substituent in the phenyl ring did not influence the hydrogen bond of the OH bound with the oxygen atom of the other OH group. Therefore, the position of the peak (at 3547 cm^{-1}) changed only by a small amount (in comparison with 3551 cm^{-1} peak of the **C**). The other peak at 3371 cm^{-1} is attributed to the stretch vibration frequency of the intramolecular hydrogen bond OH which is bound with the sulphur atom (OH···S-R). This band also is evidence for the addition of the thiols into the substituent position 6 (not position 4) in **Q**. There was no signal of the free OH. Besides these changes in the OH region, the peaks at 1666 cm^{-1} and 1690 cm^{-1} assigned to the symmetric and asymmetric C=O stretch vibrations of o-benzoquinone (figure S7b) vanish with the addition of MPA, indicating the reaction of o-benzoquinone with MPA.

The fact that there is (very) little change in the bands of the C=O of the carboxylic MPA (at 1761 cm^{-1} and 1714 cm^{-1}) shows that the C=O stretching of carboxylic acid dimers still remained after the addition reaction of MPA to o-benzoquinone. In addition, the broad band in the region 3300 – 2500 cm^{-1} remains almost unchanged, indicating that the aromatic group did not influence the formation of the carboxylic acid dimers.

However, the FT-IR results for the reaction of **Q** and MPA seem not consistent with the UV-vis measurements. While the IR spectroscopy showed that the reaction immediately occurred after o-benzoquinone was added (very fast decay of the C=O stretching mode and the appearance of the phenolic OH stretching mode within 20 minutes, that did not change versus time), the UV-vis spectra showed the slower decrease of the o-benzoquinone band at 384 nm, therefore indicating the slower reduction of o-benzoquinone. Apparently, the first fast step in the reaction (protonation

of the CO) has more dramatic influences on the IR spectrum and does not influence the UV-Vis spectrum that much.

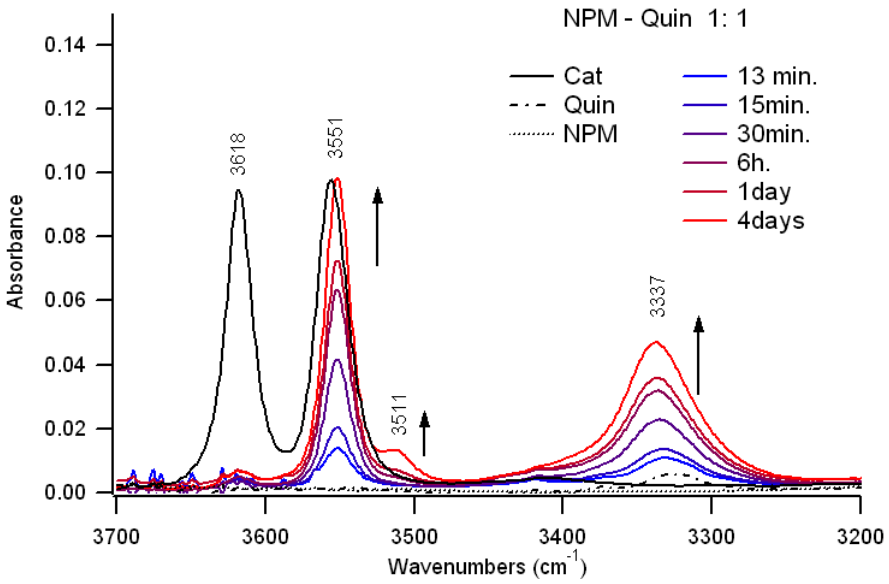

Figure S8 The FT-IR spectra of the mixture Quin (= **C**) and NPM versus time in the OH vibration region (a) and CO vibration region (b), [**C**] = [NMP] = 5×10^{-3} M, 1 mm cell thickness, CCl_4 was used as solvent. The IR spectrum of catechol (Cat = **C**, black line) is for comparison.

Figure S8 shows that the reaction of o-benzoquinone with n-propylmercaptan (NPM) was slower than the reaction with mercaptoacetic acid (MPA) because of the lower acidity of NPM, but the phenomenon is very similar. When o-benzoquinone was added, the two bands (figure S9**a**) at 3556 cm^{-1} and 3336 cm^{-1} appeared and increased in time indicating the formation of phenolic compound. The bands at 1690 cm^{-1} and 1667 cm^{-1} decreased showing the reduction of o-benzoquinone.

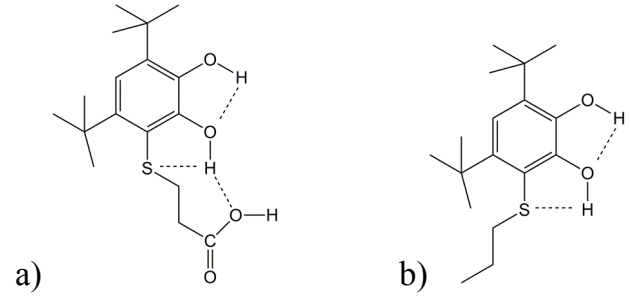

Scheme S2. The possible hydrogen bonds in 4,6-di-*tert*- butyl-3-thioalkyl-catechols, the adducts of the reaction of 3,5-di-*tert*-butyl-1,2-benzoquinone (**Q**) with MPA (a) and NPM (b).

Thus, in both cases, the reaction between o-benzoquinone and the thiols formed the phenolic compounds with the thio-group at substituent position 6. The difference in the reaction rate is due to the acidity of the thiol compounds

Reactivity of quinones with thiols probed with UV-Vis

The reactivity of **BQ** as well as that of **Q** was studied by the addition of thiol compounds. Addition of mercaptopropionic acid (MPA) into the **BQ** solution immediately resulted in a decrease in the quinone absorption band (i.e. at 388 nm). After 5 minutes, only a minor changes could be observed and within 30 min the reaction was completed. The increase of a new band at ca. 300 nm (shoulder) and two isosbestic points (at 280 and 310 nm) were observed. This indicates the formation of a new compound which is characterized by absorption bands of catechol derivatives. The red-shift of about 12 nm of the catechol band (normally at 278 nm in non-polar solvent) may be due to the influence of the thiol substituent that also broadens the absorption band (compared to **C**). We observed similar phenomena for the mixture between **Q** and MPA (or NPM, n-propylmercaptan, which reacted much slower).

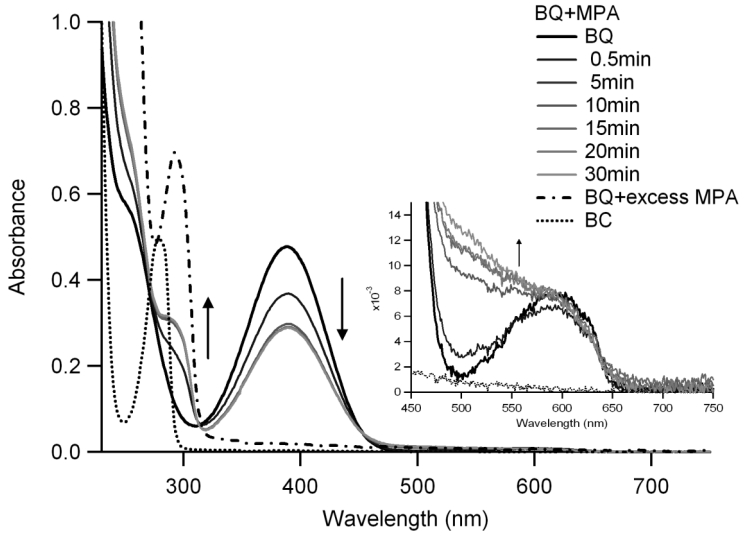

Figure S9. *The reactivity of* **BQ** *with mercapto-propionic acid (MPA) in MCH,* [**BQ**] = [MPA] = $1 \times 10^{-4}\,M$.

The addition reaction of thiols (R-SH) to 3,5-di-*tert*-butyl-1,2-benzoquinone at the *ortho*-OH position is more favorable to form 4,6-di-*tert*-butyl-3-thio-alkyl-catechols (note the change of atom numbering). The reaction of the **BQ** with thiols results in the formation of an asymmetric hemiquinone system (**AHQ**) as expressed in the following reaction (Figure S10)

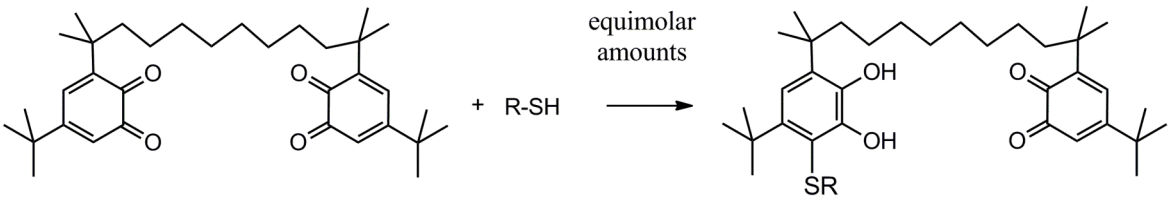

Figure S10. *Reaction of* **BQ** *with thiol compounds in equimolar ratio*.

The reaction between **Q** and thiol compounds was also studied with IR spectroscopy confirming the observations describe here.

Experimental setup, procedures and sample handling

All the solvents were purchased from Aldrich (spectroscopic or HPLC grade) and were used as received. The 3,5 di-tert-butyl o-benzoquinone (Quin = **Q**), 3,5 di-tert butyl catechol (Cat = **C**), mercaptopropinoic (MPA) and n-propyl mercaptan (NPM) were purchased from Aldrich and used without any further purification.

All samples were prepared freshly with degassed solvent and kept under argon as much as possible. The quinones are rather stable, but the catechol compounds easily oxidize (to quinones), especially in polar solvents

All experiments were performed at room temperature (21 ± 2 ˚C).

The infrared (IR) spectra were obtained using Bruker Vertex 70 FTIR spectrometers with a resolution of 1 cm^{-1}. The spectra of all samples were recorded in solution using spectroscopic grade CCl_4 as a solvent.

In nanosecond pump-probe experiments, a (Coherent) Infinity Nd: YAG-XPO laser was used for excitation. The laser illuminated a slit of 10 × 2 mm. Perpendicular to this, the probe light provided by an EG&G (FX504) low pressure Xenon lamp, irradiated the sample through a 1 mm pinhole. The overlap of the two beams fell within the first two millimeter of the cell, after the slit. The probe light from both the signal and the reference channels was then collected in optical fibers which were connected to an Acton SpectraPro-150 spectrograph which was coupled to a Princeton Instruments ICCD-576-G/RB-EM gated intensified CCD camera. Using a 5 ns gate this camera simultaneously recorded the spectrally dispersed light from both optical fibers on separate stripes of the CCD. De-aeration was performed by bubbling with Argon for 30 minutes. The UV/Vis absorption spectra of the samples were measured

before and after the laser experiments to determine any possible degradation or chemical change of the samples.

All photophysical data reported here have a 5 to 10 % error limit, unless indicated otherwise. The experiments were performed at room temperature.